Biochemical and Biophysical Research Communications 451 (2014) 252–257

Contents lists available at ScienceDirect

Biochemical and Biophysical Research Communications

journal homepage: www.elsevier.com/locate/ybbrc

Heterologous expression and solution structure of defensin from lentil *Lens culinaris* ☆

Zakhar O. Shenkarev [a], Albina K. Gizatullina [a,b], Ekaterina I. Finkina [a], Ekaterina A. Alekseeva [a], Sergey V. Balandin [a], Konstantin S. Mineev [a], Alexander S. Arseniev [a,b], Tatiana V. Ovchinnikova [a,b,*]

[a] *Shemyakin and Ovchinnikov Institute of Bioorganic Chemistry, Russian Academy of Sciences, Miklukho-Maklaya Str., 16/10, 117997 Moscow, Russia*
[b] *Moscow Institute of Physics and Technology (State University), Department of Physicochemical Biology and Biotechnology, Institutskii per., 9, 141700 Dolgoprudny, Moscow Region, Russia*

ARTICLE INFO

Article history:
Received 16 July 2014
Available online 30 July 2014

Keywords:
Antimicrobial peptide
Defensin
Lentil
Recombinant expression
Antifungal activity
NMR

ABSTRACT

A new defensin Lc-def, isolated from germinated seeds of the lentil *Lens culinaris*, has molecular mass 5440.4 Da and consists of 47 amino acid residues. Lc-def and its ^{15}N-labeled analog were overexpressed in *Escherichia coli*. Antimicrobial activity of the recombinant protein was examined, and its spatial structure, dynamics, and interaction with lipid vesicles were studied by NMR spectroscopy. It was shown that Lc-def is active against fungi, but does not inhibit the growth of Gram-positive and Gram-negative bacteria. The peptide is monomeric in aqueous solution and contains one α-helix and triple-stranded β-sheet, which form cysteine-stabilized αβ motif (CSαβ) previously found in other plant defensins. The sterically neighboring loop1 and loop3 protrude from the defensin core and demonstrate significant mobility on the μs–ms timescale. Lc-def does not bind to the zwitterionic lipid (POPC) vesicles but interacts with the partially anionic (POPC/DOPG, 7:3) membranes under low-salt conditions. The Lc-def antifungal activity might be mediated through electrostatic interaction with anionic lipid components of fungal membranes.

© 2014 Elsevier Inc. All rights reserved.

1. Introduction

Plant defensins belong to a large family of pathogenesis-related proteins (PRP), which are involved in plant defense against pests and pathogens and accumulated in plant tissues under stress conditions [1]. The defensins are basic peptides possessing antimicrobial activity toward different pathogens including bacteria, fungi, and viruses [2]. These peptides consist of 45–54 amino acid residues and characterized by the presence of some conservative amino acid residues including eight cysteines [3]. Spatial structure of plant defensins is typically formed by antiparallel triple-stranded β-sheet packed against an α-helix (in a $\beta_1\alpha\beta_2\beta_3$ configuration) [4]. Plant defensins contain three conserved intramolecular disulfide bridges (C2–C5, C3–C6, C4–C7) forming so-called cysteine-stabilized αβ motif (CSαβ) [5]. This motif was found in many toxins isolated from arthropods including arachnids and insects [5]. An additional disulfide bond (C1–C8) brings together the N- and C-terminal regions of plant defensins forming pseudo-cyclic structures.

Plant defensins possess various biological activities including inhibitory effects on a broad range of plant and human pathogens (e.g. different *Candida* species [6]), digestive enzymes (α-amylases [7] and serine proteinases [8]), HIV-1 reverse transcriptase [9], and growth of parasitic plants [10]. The peptides take part in regulating plant growth and development [11] and promote zinc tolerance in plants [12]. Some plant defensins inhibit protein translation in a cell-free system [13] and proliferation of tumor cells [14], block ion channels [15], display insecticidal effects [16] and mitogenic activity towards mouse splenocytes [17].

Molecular mechanism of antimicrobial action of plant defensins is still obscure. In contrast to other antimicrobial peptides, defensins do not permeabilize artificial phospholipid membranes [18], but induced hyphal permeabilization [19]. Recent research has demonstrated that microbe-specific lipid receptors are involved in antibiotic activity of various defensins [20]. In common with

Abbreviations: CSαβ, cysteine-stabilized αβ motif; DOPG, 1,2-dioleoyl-sn-glycero-3-phosphoglycerol; POPC, 1-palmitoyl-2-oleoyl-sn-glycero-3-phosphocholine; SUV, small unilamellar vesicles.

☆ The atomic coordinates and structure factors have been deposited in the Worldwide Protein Data Bank (PDB: 2LJ7).

* Corresponding author at: Shemyakin and Ovchinnikov Institute of Bioorganic Chemistry, Russian Academy of Sciences, Miklukho-Maklaya Str., 16/10, 117997 Moscow, Russia. Fax: +7 495 336 43 33.

E-mail addresses: ovch@ibch.ru, ovch@bk.ru (T.V. Ovchinnikova).

http://dx.doi.org/10.1016/j.bbrc.2014.07.104
0006-291X/© 2014 Elsevier Inc. All rights reserved.

human, invertebrate, and fungal defensins that bind to lipid II of the bacterial cell wall [20], plant and insect defensins were found to interact with sphingolipid receptors, resulting in fungal cell death [21]. Besides, plant defensins might enter the cell and access intracellular targets, such as DNA, RNA or components of the protein biosynthesis machinery [18].

In previous study [22], we discovered a novel defensin, termed as Lc-def, in the lentil *Lens culinaris* germinated seeds. Lc-def has molecular mass 5440.4 Da and consists of 47 amino acid residues including 8 cysteines forming 4 disulfide bonds. Here we report on the development of a bacterial expression system for production of the recombinant Lc-def and its ^{15}N-labeled analog. Antimicrobial activity and solution structure of the recombinant Lc-def were studied in the present work.

2. Materials and methods

2.1. Heterologous expression and purification of recombinant Lc-def and its ^{15}N-labeled analog

The recombinant plasmid pET-Trx-Lc-def was constructed by ligating the 5253 bp BglII/XhoI fragment of pET-31b(+) vector (Novagen) with a PCR-constructed insert encoding the recombinant protein (see Supplementary data). The BL-21 (DE3) cells transformed with pET-His8-TrxL-Lc-def were grown in LB medium containing ampicillin and glucose. ^{15}N-labeled Lc-def was expressed in M9 minimal medium containing $^{15}NH_4Cl$. Purification of the recombinant Lc-def and its ^{15}N-labeled analog involved immobilized-metal affinity chromatography (IMAC), refolding, CNBr cleavage of the fusion protein, elimination of the carrier protein by IMAC, and final RP-HPLC (see Supplementary data).

2.2. Antimicrobial assay

Antimicrobial activity of the recombinant Lc-def was measured by microspectrophotometry using 96-well microplates and serial dilutions of the peptide as described [23]. Spore germination and altered morphology of hyphae were observed with an Olympus CKX41 microscope (see Supplementary data).

2.3. NMR experiments and spatial structure calculation

NMR investigation was done using 0.5–1.0 mM samples of Lc-def or its ^{15}N-labeled analog in 10% D_2O or 100% D_2O at pH 5.0. All the NMR spectra were acquired on a Bruker Avance 600 spectrometer equipped with a cryoprobe at 27 °C or 55 °C. ^{1}H and ^{15}N resonance assignment was obtained by a standard procedure using combination of 2D and 3D TOCSY and NOESY spectra [24]. The data obtained from 2D DQF-COSY and ^{13}C-HSQC spectra were also used. The $^3J_{H^NH^\alpha}$ and $^3J_{NH^\beta}$ coupling constants were measured using 3D HNHA and HNHB experiments [24]. The $^3J_{H^\alpha H^\beta}$ coupling constants for AMX systems were estimated from splitting of $H^\alpha H^\beta$ cross-peaks in 2D TOCSY and NOESY spectra.

Spatial structure calculation was performed in the CYANA 2.1 program [25]. Upper interproton distance constraints were derived from the intensities of cross-peaks in 2D and 3D NOESY spectra (τ_m = 120 ms) via a "$1/r^6$" calibration. Torsion angle restraints and stereospecific assignments were obtained from *J* coupling constants and NOE intensities. Hydrogen bonds were introduced basing on water and deuterium exchange rates of H^N protons (Fig. 2B). The disulfide bond connectivity pattern was established on the basis of the observed NOE contacts and verified during preliminary stages of the spatial structure calculation.

^{15}N-relaxation parameters (R_1 and R_2 rates and heteronuclear ^{15}N-{^{1}H} NOEs) were measured at 27 °C using pseudo 3D experiments [24]. Hydrodynamic calculations were carried out in the HYDRONMR program [26].

Small unilamellar vesicles (SUV) composed of POPC or POPC/DOPG (7:3) mixture (Avanti Polar Lipids, Alabaster, AL) were prepared by sonication. Titration of the unlabeled Lc-def sample (30 μM, 5% D_2O, 10 mM Tris-Ac buffer, pH 7.0) with SUV was performed at 27 °C. At each lipid concentration 1D ^{1}H NMR spectrum was measured, and the equilibrium concentration of the "free" peptide in solution was determined on the basis of the integral intensity of the amide-aromatic region of the spectrum.

3. Results

3.1. Heterologous expression, purification and characterization of recombinant Lc-def and its stable isotope labeled analog

The recombinant Lc-def was produced in *Escherichia coli* using T7 promoter based expression system. *E. coli* BL-21(DE3) cells were transformed by pET-His8-TrxL-Lc-def containing the Lc-def sequence fused with the His8-tagged thioredoxin A (M37L) carrier protein (Fig. S1). Decreasing the induction temperature to 25–30 °C resulted in increasing level of the Lc-def-containing fusion protein expression in a soluble form. In LB medium the recombinant peptide was obtained mostly in a soluble form. The yield of the purified peptide constituted up to 3.5 mg/L of the medium. In order to obtain the uniformly ^{15}N-labeled recombinant Lc-def, the BL-21 (DE3) cells transformed with the same plasmid were grown in M9 minimal medium containing $^{15}NH_4Cl$ as the only source of nitrogen. The yield of the ^{15}N-labeled Lc-def was somewhat lower (2.5 mg/L). MALDI-TOF MS analysis of the recombinant Lc-def revealed a monomeric protein with molecular mass identical to that of the native defensin (5440.06 Da and 5440.4 Da, respectively). The ^{15}N-labeled Lc-def showed 73 Da increase in molecular mass (5513.69 Da) indicating that all the ^{14}N atoms were substituted with the stable isotope ^{15}N. The SDS–PAGE revealed the refolded fusion protein in a monomeric form both under reducing and non-reducing conditions. At the same time, the recombinant Lc-def demonstrated different electrophoretic mobility under reducing and non-reducing conditions. Under non-reducing conditions the main peptide band corresponded to the protein dimer (~11 kDa). Addition of an excess of 2-mercaptoethanol resulted in the appearance of a single band corresponding to the monomeric peptide (data not shown).

3.2. Biological activity of the recombinant Lc-def

Antimicrobial activity of the recombinant Lc-def against 11 phytopathogenic microorganisms was examined by the broth

Table 1
Antimicrobial activity of Lc-def.

Test-microorganisms[a]	IC_{50}, μM
Bacteria	
Agrobacterium tumefaciens, strain A281	NA
Clavibacter michiganensis, strain VKM Ac-1144	NA
Pseudomonas syringae, strain VKM B-1546	NA
Fungi	
Alternaria alternata, strain VKM F-3047	NA
Ascochyta pisi, strain VKM F-1173	NA
Aspergillus niger, strain VKM F-2259	18.5
Aspergillus versicolor, strain VKM F-1114	18.5
Botrytis cinerea, strain VKM F-3700	9.25
Fusarium culmorum, strain VKM F-844	18.5–37.0
Fusarium solani, strain VKM F-142	NA
Neurospora crassa, strain VKM F-184	9.25–18.5

NA, not active.
[a] VKM strains were from all-Russian collection of microorganisms.

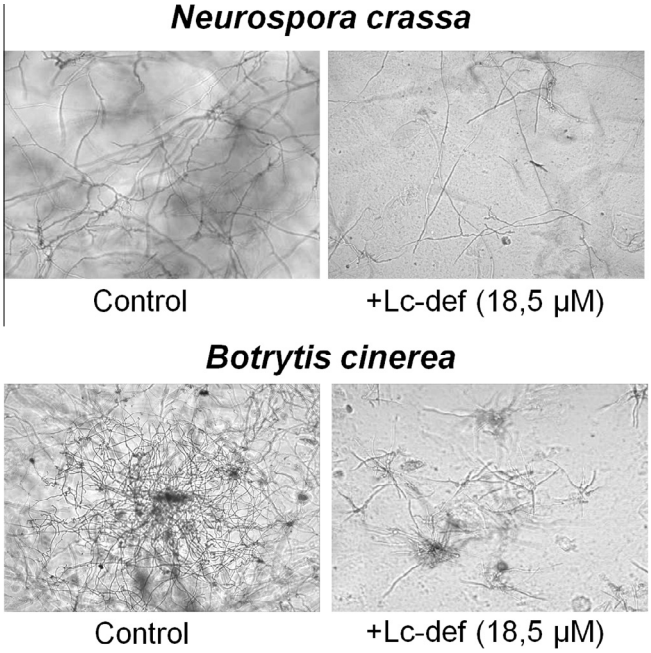

Fig. 1. Effect of Lc-def on the growth of *N. crassa* and *B. cinerea* (×100 magnification).

microdilution assay (Table 1). The defensin exhibited antifungal activity, but did not inhibit the growth of Gram-positive or Gram-negative bacteria. Similarly to other plant defensins [27], the observed antifungal activity of Lc-def strongly depends on the targeted fungus. The fungi *Botrytis cinerea* and *Neurospora crassa* were the most sensitive test microorganisms to Lc-def (Fig. 1). Effectiveness of Lc-def against *N. crassa* was nearly 100% after 48 h at the peptide concentration of 37 μM. At the same time, Lc-def almost did not inhibit the growth of such fungi as *Alternaria alternata*, *Ascochyta pisi*, and *Fusarium solani* at the maximal tested concentration of 37 μM. Microscopic analysis showed that Lc-def not only inhibited the *N. crassa* and *B. cinerea* spore germination, but also altered the morphology of their hyphae at the peptide concentration of 18.5 μM (Fig. 1). The defensin inhibited hyphal growth with a concomitant increase in hyphal branching. In addition, Lc-def at high concentrations ($\geqslant$37 mM) induced lysis of the fungus mycelium.

3.3. Optimization of conditions for NMR study

Preliminary NMR spectra of the ^{15}N-labeled Lc-def measured at pH 3.5 and 27 °C revealed significantly inhomogeneous distribution of line-widths and peak intensities for the signals of HN groups (data not shown). The observed line broadening pointed to the presence of conformational exchange process(es) taking place on the μs–ms timescale. To find optimal conditions for the NMR study, several parameters including temperature, pH and ionic strength were systematically varied in the ranges of 10–55 °C, pH 3.0–7.0 and 0–100 mM, respectively. Variation in pH and ionic strength did not significantly affect quality of the NMR spectra. Increase in the temperature above 50 °C (at pH $\geqslant$ 5.0) resulted in narrowing of some sets of HN signals, but induced broadening of some other signals, probably due to acceleration of the exchange with water. pH 5.0 and 27 °C in the absence of salt were chosen as optimal conditions for the structural study. At these conditions only 36 of 44 expected backbone HN groups were observed in the ^{15}N-HSQC spectrum (Fig. 2A and B, lower row). Complementary NMR spectra were acquired at 55 °C. In spite of thorough conditions optimization, the spin systems corresponding to the residues Cys14-Cys20 were not identified at any conditions tested.

3.4. Spatial structure and backbone dynamics of Lc-def

According to the obtained NMR data (Fig. 2B) and the calculated set of spatial structures (Fig. 3A, Table S1) the secondary structure of Lc-def involves triple-stranded antiparallel β-sheet (Lys1-Leu6, Ser32-Cys35, Cys41-Cys47) and one α-helical region (Asn21-Lys27). These results are in good agreement with the circular dichroism data (Fig. S2), indicating that Lc-def contains about 33% of β-sheet and 16% of α-helix. The peptide structure is stabilized by four disulfide bonds (Cys3-Cys47, Cys14-Cys35, Cys20-Cys41 and Cys24-Cys43) and 16 hydrogen bonds. The calculated Lc-def structure is well defined in the regions corresponding to secondary structure elements (β-sheet and α-helix). At the same time,

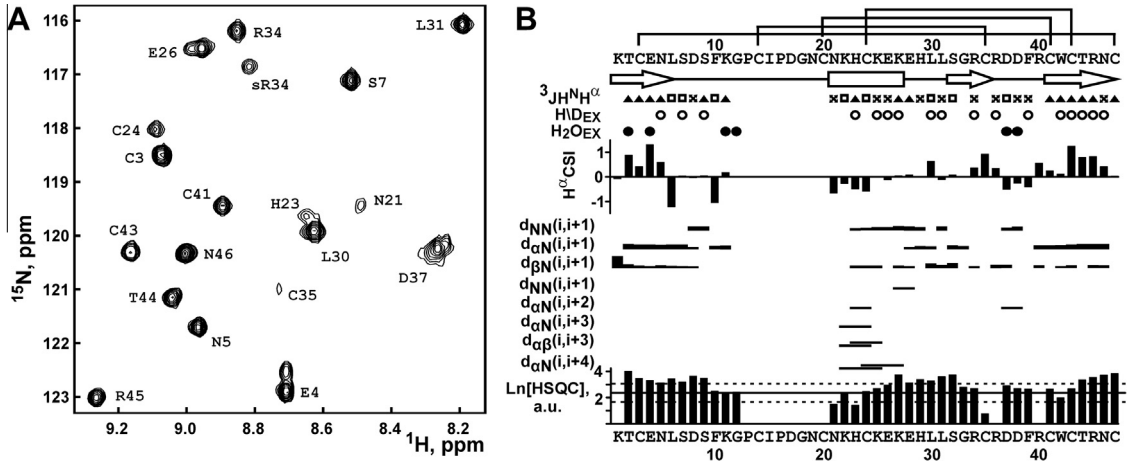

Fig. 2. (A) The fragment of 2D ^{15}N-HSQC spectrum of 0.5 mM Lc-def at pH 5.0 and 27 °C. The resonances of side chain groups are marked with subscript "s". (B) Overview of the NMR data collected for Lc-def. (From top to bottom.) Large (>8 Hz), small (<6 Hz) and medium (others) $^{3}J_{H^{N}H^{\alpha}}$ couplings are indicated by the filled triangles, open squares, and crosses, respectively. The open circles (H/D$_{EX}$) denote H^{N} protons with H-D half-exchange time > 30 min. Amide protons which demonstrate fast exchange with water protons are shown by filled circles (H$_2$O$_{EX}$). The corresponding cross-peaks on the water frequency were observed in the 3D ^{15}N-TOCSY-HSQC spectrum (τ_m 80 ms). H$^{\alpha}$ chemical shift indices (H$^{\alpha}$CSI), positive and negative values correspond to β-structure and α-helix, respectively. NOE connectivities correspond to cross-peaks observed in the 120 ms 2D and 3D NOESY spectra. (Ln[HSQC]) – intensity (log values) of peaks in ^{15}N-HSQC spectrum. The level corresponding to the average intensity is shown by a solid line. The levels corresponding to twice smaller or twice larger intensities are shown by broken lines.

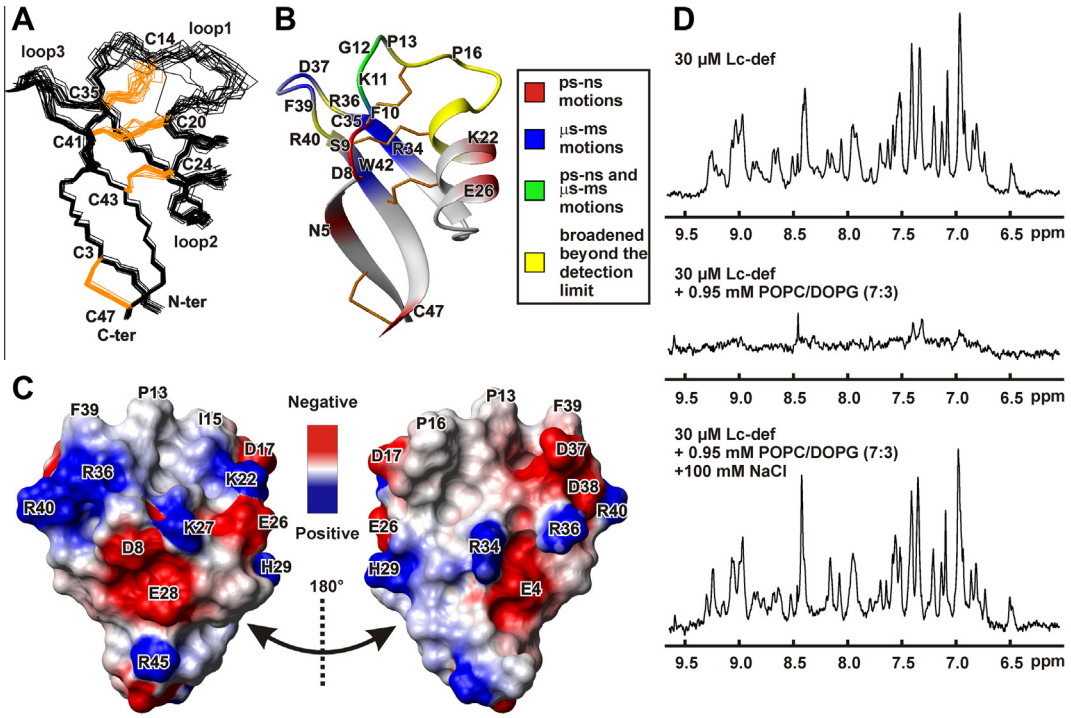

Fig. 3. (A) The calculated set of the 20 Lc-def structures. (B) Spatial structure and backbone dynamics of Lc-def in aqueous solution. The peptide ribbon is colored according to the dynamical NMR data obtained from the ^{15}N-relaxation measurements (see legend, experimental data are presented in Fig. S3). Residues with the significantly broadened HN signals (pH 5.0 and 27 °C) are shown in yellow. This broadening is the consequence of the μs–ms exchange process(es). (C) Two-sided view of electrostatic potential on the Lc-def surface. (D) Lc-def binding to POPC/DOPG (7:3) vesicles (10 mM Tris-Ac, pH 7.0, 27 °C). (For interpretation of the references to color in this figure legend, the reader is referred to the web version of this article.)

conformations of two loops (loop1 and loop3) protruding from the defensin core and the N-terminal turn of the α-helix (residues Lys11-Cys21 and Asp37-Arg40) remain loosely defined (Fig. 3A). The lack of structural convergence is connected with the absence of observable NMR signals or significant line broadening in the mentioned above regions of the molecule (Fig. 2B).

The ^{15}N relaxation data (Fig. S3) were used to characterize mobility of the peptide backbone on ps–ns and μs–ms timescales. Interpretation of the obtained data (for example, with the use of so-called "model free" approach [24]) turned out to be a problem due to the presence of significant μs–ms exchange contributions to the R_2 relaxation rates for 8 HN groups of the 36 observed ones (Fig. S4). However, qualitative analysis revealed that some amino acid residues in the N-terminal β-strand, loop1, α-helix and the C-terminal Cys47 are probably subjected to extensive motions on the ps–ns timescale (Fig. 3B, red and green). These residues demonstrate heteronuclear ^{15}N-{^{1}H} NOE values < 0.55. On the other hand, spatially neighboring fragments including the loop1, the N-terminal turn of the α-helix, the second and third β-strands, and the loop3 are mobile on the μs–ms timescale (Fig. 3B, blue, green and yellow). These residues either were unobservable in the NMR spectra (probably their broadened beyond the detection limit) or demonstrated elevated values of relaxation rates R_2 and effective rotational correlation times τ_R (calculated from R_2/R_1 ratio, see Fig. S3). It should be noted that the loop1 contains two Pro residues (13 and 16), and possible *cis–trans* isomerization of the Xxx-Pro peptide bonds might contribute to the observed μs–ms dynamics. The average τ_R value (2.8 ns) calculated over "stable" regions of the peptide (Fig. S3) is in good correspondence with the results of hydrodynamic calculations (2.9 ns) carried out with the use of experimentally determined spatial structure of Lc-def. These data indicate that Lc-def is monomeric in aqueous solution.

3.5. Interaction of Lc-def with lipid vesicles

The maps of electrostatic (Fig. 3C) and molecular hydrophobicity (Fig. S4) potentials showed that the positive and negative charges are distributed uniformly on the quite hydrophilic Ls-def surface (net charge of the peptide is +2). The defensin does not contain evident hydrophobic patches that could contribute to membrane anchoring or inserting. Nevertheless, the side chains of Pro13, Ile15, Pro16, and Phe39 residues (loop1 and loop3) form a small stretched nonpolar cluster (Fig. 3C). To investigate membrane binding propensity of Lc-def, the vesicles consisting of either zwitterionic lipids (POPC) or the mixture of anionic and zwitterionic lipids (POPC/DOPG 7:3) were added to the water solution of Lc-def, and quantity of the unbound peptide was estimated by ^{1}H NMR (Fig. 3D and Fig. S5). It was found that the peptide does not bind to the zwitterionic membranes but interact with the partially anionic vesicles in the absence of salt. Addition of 100 mM NaCl caused a complete release of the bound Lc-def from the liposomes (Fig. 3D).

4. Discussion

In this report Lc-def has been shown to possess highly specific antimicrobial activity. The peptide exhibits antifungal activity, but does not inhibit growth of Gram-positive and Gram-negative bacteria. Microscopic analysis revealed that Lc-def belongs to a subgroup of morphogenic plant defensins which inhibit hyphal growth with a concomitant increase in hyphal branching. Mode of antifungal action of plant defensins is still needs to be unraveled. Being the cationic peptides, defensins may directly interact with the negatively charged microbial membranes, form the ionic channels or transmembrane pores and induce lysis of the target cell

[28]. On the other hand, antifungal defensins may interact with specific component of the plasma membrane, penetrate into the cell, and interact with intracellular targets [21,29]. In this case the defensin action might be mediated by intracellular formation of reactive oxygen species and programmed cell death [21]. To propose a mechanism of antifungal action of the lentil defensin, biophysical and structural investigations were performed here.

Plant defensins demonstrate low similarity in amino acid sequences; only a few residues including eight cysteines, Gly at positions 12 and 33, Phe/Tyr/Trp10, Ser7, and Glu28 are highly conserved (the sequential numbering is relative to Lc-def). Despite low identity in primary structures, defensins share similar three-dimensional scaffold – CSαβ motif. The structural data, presently obtained by heteronuclear ^{1}H,^{15}N NMR spectroscopy, showed that the Lc-def core adopted well-ordered and compact CSαβ-type structure. The peptide contains α-helix, three antiparallel β-strands (β1–3) and two extended loops (Fig. 3B). These loops protrude from the Lc-def core (the loop1 connects β1 with the α-helix, and the loop3 couples β2 with β3) and demonstrate significant mobility on the μs–ms timescale. These loops are fastened together by the disulfide bond Cys14-Cys35. Interestingly, the region of enhanced mobility also covers the adjacent fragments of the α-helix and β-strands (Fig. 3B).

As peptide-membrane interactions might be involved in antimicrobial action of plant defensins [19], lipid-binding propensity of Lc-def was evaluated. Zwitterionic and anionic lipid vesicles were used as model membranes. Lc-def was able to bind anionic vesicles under low-salt conditions, but did not interact with them at the physiological ionic strength (100 mM NaCl). These data are in line with the absence of the tested antibacterial activity and suggest that specific target might be involved in Lc-def interaction with the fungal membranes. The presence of the "dynamic" region on the Lc-def surface implies that the defensin loop1 and loop3 may form the binding site. This proposal is in agreement with the results obtained for other plant defensins. For example, the loop3 was reported as a major determinant of antifungal activity of the radish defensin Rs-AFP2 [30]. This activity was mediated by the peptide interaction with glucosylceramides from fungal membranes [29]. At the same time, the sequence of the Lc-def loop3 (C_{35}RDDFRC$_{41}$) has no homology with that of Rs-AFP2 (C_{36}NYVFPAHKC$_{45}$), thus indicating involvement of other membrane receptor or mechanism. Similarly to Lc-def, the enhanced μs–ms mobility was observed in the loop1 of pea antifungal defensin Psd1 [31]. The region of enhanced mobility also covered the N-terminal turn of the Psd1 α-helix. As reported, this Psd1 fragment is responsible for the defensin interaction with glucosylceramide from *F. solani*. Low sequence homology in the corresponding loops of Psd1 and Lc-def (Y_{10}RGVCFTNASC$_{20}$ and F_{10}-KGPCIPDGNC$_{20}$, respectively) also argues for targeting different membrane receptors.

It was observed that some plant defensins tend to form dimers [27]. Recently, the dimeric state of the antifungal defensin SPE10 from *Pachyrrhizus erosu* was shown by X-ray crystallography [32]. The asymmetric dimer is formed by association of the loop3 and β3 residues (R36, R40, and W42) of one monomer with the α-helix of another. In spite of the fact that Lc-def has similar R36, R40, and W42 residues, the presently obtained ^{15}N-relaxation data indicate that the lentil defensin is monomeric in aqueous solution. The observed difference is probably related to the essential sequence difference in the α-helical regions, where SPE10 contains a lot of acidic residues in contrast with Lc-def. Interestingly, the formation of Lc-def dimers was observed in the SDS–PAGE under non-reducing conditions. Previously, similar behavior was documented for the cationic antimicrobial peptide arenicin-2 from the marine polychaeta *Arenicola marina* [33] which was able to form oligomeric pores in planar lipid bilayers [34].

In summary, we characterized a new defensin Lc-def from germinated seeds of lentil *L. culinaris* by biological and structural methods. It was observed that Lc-def displays antifungal activity, adopts CSαβ motif and is able to interact with the anionic lipid membranes under low-salt conditions. Presumably, antifungal activity of the lentil defensin is mediated through electrostatic interaction with anionic lipid components of fungal membranes. Our results afford further molecular insight into possible mechanism of antifungal action of plant defensins.

Acknowledgment

The reported study was partially supported by the Russian Foundation for Basic Research (Project No. 12-04-01224).

Appendix A. Supplementary data

Supplementary data associated with this article can be found, in the online version, at http://dx.doi.org/10.1016/j.bbrc.2014.07.104.

References

[1] J. Sels, J. Mathys, B.M. de Coninck, B.P. Cammue, M.F. de Bolle, Plant pathogenesis-related (PR) proteins: a focus on PR peptides, Plant Physiol. Biochem. 46 (2008) 941–950.
[2] Ade O. Carvalho, V.M. Gomes, Plant defensins – prospects for the biological functions and biotechnological properties, Peptides 30 (2009) 1007–1020.
[3] N.L. van der Weerdena, M.A. Anderson, Plant defensins: common fold, multiple functions, Fungal Biol. Rev. 26 (2013) 121–131.
[4] F. Fant, W.F. Vranken, F. Borremans, The three-dimensional solution structure of *Aesculus hippocastanum* antimicrobial protein 1 determined by 1H nuclear magnetic resonance, Proteins 37 (1999) 388–403.
[5] Y. Kobayashi, H. Takashima, H. Tamaoki, Y. Kyogoku, P. Lambert, H. Kuroda, N. Chino, T.X. Watanabe, T. Kimura, S. Sakakibara, L. Moroder, The cystine-stabilized alpha-helix: a common structural motif of ion-channel blocking neurotoxic peptides, Biopolymers 31 (1991) 1213–1220.
[6] P.M. Tavares, K. Thevissen, B.P. Cammue, I.E. François, E. Barreto-Bergter, C.P. Taborda, A.F. Marques, M.L. Rodrigues, L. Nimrichter, In vitro activity of the antifungal plant defensin RsAFP2 against *Candida* isolates and its *in vivo* efficacy in prophylactic murine models of candidiasis, Antimicrob. Agents Chemother. 52 (2008) 4522–4525.
[7] N. Zhang, B.L. Jonnes, H.P. Tao, Purification and characterization of a new class of insect α-amylase inhibitors from barley, Cereal Chem. 74 (1997) 119–122.
[8] R. Wijaya, G. Neumann, R. Condor, A. Hughes, G. Polya, Defense proteins from seed of *Cassia fistula* include a lipid transfer protein homologous and a protease inhibitory plant defensing, Plant Sci. 159 (2000) 243–255.
[9] J.H. Wong, T.B. Ng, Limenin, a defensin-like peptide with multiple exploitable activities from shelf beans, J. Pept. Sci. 12 (2006) 341–346.
[10] A. De Zelicourt, P. Letousey, S. Thoiron, C. Campion, P. Simoneau, K. Elmorjani, D. Marion, P. Simier, P. Delavault, Ha-DEF1, a sunflower defensin, induces cell death in *Orobanche* parasitic plants, Planta 226 (2007) 591–600.
[11] A. Allen, A.K. Snyder, M. Preuss, E.E. Nielsen, D.M. Shah, T.J. Smith, Plant defensins and virally encoded fungal toxin KP4 inhibit plant root growth, Planta 227 (2008) 331–339.
[12] M. Mirouze, J. Sels, O. Richard, P. Czernic, S. Loubet, A. Jacquier, I.E. François, B.P. Cammue, M. Lebrun, P. Berthomieu, L. Marquès, A putative novel role for plant defensins: a defensin from the zinc hyper-accumulating plant, *Arabidopsis halleri*, confers zinc tolerance, Plant J. 47 (2006) 329–342.
[13] E. Mendez, A. Moreno, F. Colilla, F. Pelaez, G.G. Limas, R. Mendez, F. Soriano, M. Salinas, C. de Haro, Primary structure and inhibition of protein synthesis in eukaryotic cell-free system of a novel thionin, gamma-hordothionin, from barley endosperm, Eur. J. Biochem. 194 (1990) 533–539.
[14] J.H. Wong, T.B. Ng, Sesquin, a potent defensin-like antimicrobial peptide from ground beans with inhibitory activities toward tumor cells and HIV-1 reverse transcriptase, Peptides 26 (2005) 1120–1126.
[15] C. Kushmerick, C.M. De Souza, C.J. Santos, C.J. Bloch, P.S. Beirao, Functional and structural features of gamma-zeathionins, a new class of sodium channel blockers, FEBS Lett. 440 (1998) 302–306.
[16] K.C. Chen, C.Y. Lin, C.C. Kuan, H.Y. Sung, C.S. Chen, A novel defensin encoded by a mungbean cDNA exhibits insecticidal activity against bruchid, J. Agric. Food Chem. 50 (2002) 7258–7263.
[17] P.H. Ngai, T.B. Ng, Phaseococcin, an antifungal protein with antiproliferative and anti-HIV-1 reverse transcriptase activities from small scarlet runner beans, Biochem. Cell Biol. 83 (2005) 212–220.
[18] A.M. Aerts, I.E. François, B.P. Cammue, K. Thevissen, The mode of antifungal action of plant, insect and human defensins, Cell. Mol. Life Sci. 65 (2008) 2069–2079.

[19] K. Thevissen, F.R. Terras, W.F. Broekaert, Permeabilization of fungal membranes by plant defensins inhibits fungal growth, Appl. Environ. Microbiol. 65 (1999) 5451–5458.
[20] M. Wilmes, B.P. Cammue, H.G. Sahl, K. Thevissen, Antibiotic activities of host defense peptides: more to it than lipid bilayer perturbation, Nat. Prod. Rep. 28 (2011) 1350–1358.
[21] K. Thevissen, I.E. Francois, J.Y. Takemoto, K.K. Ferket, E.M. Meert, B.P. Cammue, DmAMP1, an antifungal plant defensin from dahlia (*Dahlia merckii*), interacts with sphingolipids from *Saccharomyces cerevisiae*, FEMS Microbiol. Lett. 226 (2003) 169–173.
[22] E.I. Finkina, E.I. Shramova, A.A. Tagaev, T.V. Ovchinnikova, A novel defensin from the lentil *Lens culinaris* seeds, Biochem. Biophys. Res. Commun. 371 (2008) 860–865.
[23] A.K. Gizatullina, E.I. Finkina, K.S. Mineev, D.N. Melnikova, I.V. Bogdanov, I.N. Telezhinskaya, S.V. Balandin, Z.O. Shenkarev, A.S. Arseniev, T.V. Ovchinnikova, Recombinant production and solution structure of lipid transfer protein from Lentil *Lens culinaris*, Biochem. Biophys. Res. Commun. 439 (2013) 427–432.
[24] J. Cavanagh, W.J. Fairbrother, A.G. Palmer, N.J. Skelton, M. Rance, Protein NMR Spectroscopy Principles and Practice, second ed., Academic Press, New York, 2006.
[25] P. Guntert, Automated NMR structure calculation with CYANA, Method Mol. Biol. 278 (2004) 353–378.
[26] J. García de la Torre, M.L. Huertas, B. Carrasco, HYDRONMR: prediction of NMR relaxation of globular proteins from atomic-level structures and hydrodynamic calculations, J. Magn. Reson. 147 (2000) 138–146.
[27] X. Song, J. Wang, F. Wu, X. Li, M. Teng, W. Gong, CDNA cloning, functional expression and antifungal activities of a dimeric plant defensing SPE10 from *Pachyrrhizus erosus* seeds, Plant Mol. Biol. 57 (2005) 13–20.
[28] B.L. Kagan, M.E. Selsted, T. Ganz, R.I. Lehrer, Antimicrobial defensin peptides form voltage-dependent ion-permeable channels in planar lipid bilayer membranes, Proc. Natl. Acad. Sci. U.S.A. 87 (1990) 210–214.
[29] K. Thevissen, D.C. Warnecke, I.E. Francois, M. Leipelt, E. Heinz, C. Ott, U. Zahringer, B.P. Thomma, K.K. Ferket, B.P. Cammue, Defensins from insects and plants interact with fungal glucosylceramides, J. Biol. Chem. 279 (2004) 3900–3905.
[30] W.M.M. Schaaper, G.A. Posthuma, R.H. Meloen, H.H. Plasman, L. Sijtsma, A. Van Amerongen, F. Fant, F.A.M. Borremans, K. Thevissen, W.F. Broekaert, Synthetic peptides derived from the β2−β3 loop of *Raphanus sativus* antifungal protein 2 that mimic the active site, J. Peptide Res. 57 (2001) 409–418.
[31] L.N. de Medeiros, R. Angeli, C.G. Carzedas, E. Barreto-Bergter, A.P. Valente, E. Kurtenbach, F.C. Almeida, Backbone dynamics of the antifungal Psd1 pea defensin and its correlation with membrane interaction by NMR spectroscopy, Biochim. Biophys. Acta 1798 (2010) 105–113.
[32] X. Song, M. Zhang, Z. Zhou, W. Gong, Ultra-high resolution crystal structure of a dimeric defensin SPE10, FEBS Lett. 585 (2011) 300–306.
[33] T.V. Ovchinnikova, Z.O. Shenkarev, S.V. Balandin, K.D. Nadezhdin, A.S. Paramonov, V.N. Kokryakov, A.S. Arseniev, Molecular insight into mechanism of antimicrobial action of the beta-hairpin peptide arenicin: specific oligomerization in detergent micelles, Biopolymers 89 (2008) 455–464.
[34] Z.O. Shenkarev, S.V. Balandin, K.I. Trunov, A.S. Paramonov, S.V. Sukhanov, L.I. Barsukov, A.S. Arseniev, T.V. Ovchinnikova, Molecular mechanism of action of β-hairpin antimicrobial peptide arenicin: oligomeric structure in dodecylphosphocholine micelles and pore formation in plasnar lipid bilayers, Biochemistry 50 (2011) 6255–6265.